

Geophysical Research Letters[®]



RESEARCH LETTER

10.1029/2025GL121289

Machine Learning Eliminates Reanalysis Warm Bias and Reveals Weaker Winter Surface Cooling Over Arctic Sea Ice

Key Points:

- Bias correcting ERA5 with a neural network reduces RMSE for net shortwave by ~40%, 2 m temperature by ~34% and surface energy budget by ~55%
- Bias-correction eliminates the wintertime warm bias of about 4 K in ERA5 and reduces wintertime surface cooling by about 50%
- Corrected data capture the observed clear and cloudy states of the Arctic winter boundary layer

Supporting Information:

Supporting Information may be found in the online version of this article.

Correspondence to:

A. Hossain,
akil.hossain@awi.de

Citation:

Hossain, A., Keil, P., Grover, H., Brooks, I. M., Cox, C. J., Gallagher, M. R., et al. (2026). Machine learning eliminates reanalysis warm bias and reveals weaker winter surface cooling over Arctic sea ice. *Geophysical Research Letters*, 53, e2025GL121289. <https://doi.org/10.1029/2025GL121289>

Received 17 DEC 2025

Accepted 23 MAY 2026

Author Contributions:

Conceptualization: Felix Pithan

Data curation: Ian M. Brooks, Christopher J. Cox, Michael R. Gallagher, Mats A. Granskog, Heather Guy, Stephen R. Hudson, P. Ola G. Persson, Matthew D. Shupe, Michael Tjernström, Jutta Vüllers, Von P. Walden



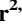



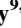




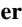


Formal analysis: Akil Hossain, Felix Pithan

Funding acquisition: Felix Pithan

Investigation: Akil Hossain, Paul Keil, Harsh Grover, Felix Pithan

Methodology: Akil Hossain, Paul Keil, Harsh Grover

Supervision: Felix Pithan

Akil Hossain¹ , Paul Keil^{2,3,4} , Harsh Grover^{2,3,4} , Ian M. Brooks⁵ , Christopher J. Cox⁶ , Michael R. Gallagher^{6,7} , Mats A. Granskog⁸ , Heather Guy^{9,10} , Stephen R. Hudson⁸ , P. Ola G. Persson^{6,7} , Matthew D. Shupe^{6,7} , Michael Tjernström¹¹ , Jutta Vüllers¹², Von P. Walden¹³ , and Felix Pithan^{1,14} 

¹Alfred Wegener Institute, Helmholtz Centre for Polar and Marine Research, Bremerhaven, Germany, ²Helmholtz Centre Hereon, Geesthacht, Germany, ³Helmholtz AI, Munich, Germany, ⁴Deutsches Klimarechenzentrum GmbH (DKRZ), Hamburg, Germany, ⁵Institute for Climate & Atmospheric Science, School of Earth & Environment, University of Leeds, Leeds, UK, ⁶National Oceanic and Atmospheric Administration (NOAA) Physical Sciences Laboratory (PSL), Boulder, CO, USA, ⁷Cooperative Institute for Research in Environmental Sciences (CIRES), University of Colorado, Boulder, CO, USA, ⁸Norwegian Polar Institute, Fram Centre, Tromsø, Norway, ⁹National Centre for Atmospheric Science, Leeds, UK, ¹⁰School of Earth and Environment, University of Leeds, Leeds, UK, ¹¹Department of Meteorology & Bolin Centre for Climate Research, Stockholm University, Stockholm, Sweden, ¹²Institute of Meteorology and Climate Research Atmospheric Trace Gases and Remote Sensing (IMKASF), Karlsruhe Institute of Technology (KIT), Karlsruhe, Germany, ¹³Department of Civil and Environmental Engineering, Laboratory for Atmospheric Research, Washington State University, Pullman, WA, USA, ¹⁴Institute of Environmental Physics, University of Bremen, Bremen, Germany

Abstract The surface energy budget governs Arctic sea-ice growth/melt, yet observations are sparse, and reanalysis data sets suffer from systematic biases. Here, we train a neural network with observational data to bias-correct hourly ERA5 fluxes over Arctic ice-covered regions ($\geq 70^\circ\text{N}$; sea-ice concentration $> 80\%$) for 1994–2024. Training data cover two full seasonal cycles and different sea-ice regimes. The neural network reduces RMSE for net shortwave radiation by ~40%, downward longwave radiation by ~16% and the total surface energy budget by ~55%, eliminating the wintertime warm bias of ~4 K in ERA5. Wintertime surface cooling is reduced by ~50%, yielding thermodynamic ice-growth estimates of ~80–120 cm, consistent with SMOS–CryoSat satellite thickness increases and in contrast to the 150–200 cm growth implied by ERA5. Our bias-corrected data capture the observed clear/cloudy states of the winter boundary layer and can be used to study Arctic climatology, evaluate climate models and drive sea-ice-ocean models.

Plain Language Summary The Arctic Ocean is warming rapidly, and its shrinking sea-ice cover is strongly influenced by exchange of heat between the atmosphere and ice surface. Correctly estimating this energy exchange is crucial for understanding how quickly sea-ice grows in winter and melts in summer. However, direct surface flux measurements over Arctic sea-ice are sparse, and widely used ERA5 reanalysis data contain persistent errors in surface fluxes and near-surface temperature. We use observations from major Arctic field campaigns to train a machine-learning model that corrects these errors. The resulting data set SEBai substantially improves estimates of surface fluxes and 2 m temperature. It reduces errors by 40% for sunlight absorbed at the surface, and more than half for the total surface energy budget. It removes the 4°C winter warm bias in ERA5. These improvements point to a reduced wintertime cooling and weaker summertime heating, suggesting that Arctic sea-ice may be more vulnerable to climate change than ERA5 implies. SEBai also reproduces the observed clear and cloudy winter states that strongly affect thermal infrared radiation but are poorly represented in ERA5. SEBai provides a more reliable baseline for climate model evaluation, Arctic climate studies, and driving sea-ice-ocean models.

1. Introduction

The surface energy budget (SEB), or more precisely the surface component of the atmospheric energy budget, summarizes the exchanges of turbulent (sensible and latent heat) and radiative (shortwave and longwave) fluxes between the atmosphere and the underlying land, sea-ice or ocean surface (Andrews et al., 2009). From the surface perspective, these terms are often referred to as the atmosphere-surface flux, while the full SEB additionally includes subsurface conductive flux. Seasonal imbalances in the SEB control sea-ice melt in summer and ice growth in winter (Persson et al., 2002). The near-surface temperature, which is the most important indicator of

© 2026. The Author(s).

This is an open access article under the terms of the [Creative Commons Attribution License](https://creativecommons.org/licenses/by/4.0/), which permits use, distribution and reproduction in any medium, provided the original work is properly cited.

Validation: Akil Hossain, Paul Keil, Harsh Grover
Visualization: Akil Hossain, Felix Pithan
Writing – original draft: Akil Hossain
Writing – review & editing: Paul Keil, Harsh Grover, Ian M. Brooks, Christopher J. Cox, Michael R. Gallagher, Mats A. Granskog, Heather Guy, Stephen R. Hudson, P. Ola G. Persson, Matthew D. Shupe, Michael Tjernström, Jutta Vuöllers, Felix Pithan

global-mean and amplified Arctic climate change (Rantanen et al., 2022), is closely related to the surface fluxes. Understanding the state of the near-surface atmosphere and the SEB and accurately representing them in models is thus essential for understanding Arctic climate variability and climate change (Serreze et al., 2007; Taylor et al., 2022).

Despite its vital role, the SEB in the Arctic remains poorly constrained. Direct in situ observations over sea-ice are sparse (Jung et al., 2016). They are temporally intermittent and challenged by extreme environmental conditions. Beyond the Multidisciplinary drifting Observatory for the Study of Arctic Climate (MOSAiC; Shupe et al., 2022) and Surface Heat Budget of the Arctic Ocean (SHEBA; Uttal et al., 2002) drift campaigns, each covering a full seasonal cycle on drifting sea-ice, only shorter timeseries of a few weeks or months are available. Satellite retrievals provide broad spatial coverage, but their use is constrained by cloud contamination uncertainties (Li et al., 2022; Müller & Pfeifroth, 2022) and difficulties in distinguishing between snow, sea-ice, and open water surfaces (Istomina et al., 2020; Wernecke et al., 2024).

Consequently, atmospheric reanalysis data has become crucial for studying the Arctic climate and SEB (Jakobson et al., 2012). While these data sets have full spatial and temporal coverage, they still suffer from the lack of in situ observations and difficulties in assimilating satellite data, in particular in Arctic winter (Lawrence et al., 2019). Model biases in the representation of stable boundary layers (Sandu et al., 2013), mixed-phase clouds (Pithan et al., 2016) and snow on sea-ice (Batra & Müller, 2019) add to these difficulties.

Reanalysis data, including the widely used ERA5 product from the European Centre for Medium-Range Weather Forecasts (ECMWF; Hersbach et al., 2020), therefore exhibit substantial and systematic biases in near-surface temperature, turbulent and radiative fluxes over Arctic sea-ice (Batra & Müller, 2019; Di Biagio et al., 2021; Graham et al., 2019). In particular, ERA5 is known to suffer from a near-surface warm bias of several degrees in cold winter conditions (Batra & Müller, 2019) and does not reproduce the observed bimodal distribution of surface net longwave radiation in Arctic winter (Bertossa et al., 2025).

In recent years, machine learning (ML) has emerged as a powerful tool for improving climate data products. ML-based bias correction methods have been applied to temperature (Moghimi & Bras, 2017; Niazkar et al., 2024; Zampieri et al., 2023), precipitation (Li et al., 2023; Sun et al., 2022), surface downwelling shortwave radiative flux (Mallet et al., 2023) and other radiation (Clark et al., 2022) fields. The potential of ML to bias-correct the Arctic SEB in reanalyses is yet to be explored.

In this study, we bias-correct ERA5 surface energy fluxes over the Arctic Ocean using a simple feed-forward neural network (NN). The NN learns the relationship between the state of the atmosphere as represented in ERA5 and the observed surface fluxes, and uses this relationship to deduce more realistic surface fluxes even in the absence of observations. We utilize 16 meteorological ERA5 variables as input and observations from the MOSAiC, SHEBA, Arctic Ocean 2018 (AO2018; Vuöllers et al., 2021), Norwegian young sea ICE (N-ICE2015; Granskog et al., 2018) and ARTofMELT (Tjernström & Zieger, 2025) expeditions as ground truth during training. Model robustness is assessed using a leave-one-campaign-out cross-validation framework, in which each campaign is withheld in turn, with N-ICE2015 additionally used as a primary case for detailed evaluation.

Our NN (a) substantially reduces systematic SEB biases in the reanalysis, (b) eliminates the wintertime near-surface warm bias, and (c) produces half as much wintertime cooling and weaker summertime heating than ERA5, resulting in a weaker amplitude of the seasonal cycle of the SEB.

2. Methods

2.1. Observational Data

We use the observational data sets from the MOSAiC, SHEBA, N-ICE2015, AO2018 and ARTofMELT (Figure S1–S2 in Supporting Information S1) field campaigns. MOSAiC is a year-long (October 2019–October 2020) drift expedition in the central Arctic Ocean. We apply the final processed data from the central “Met City” 10-m meteorological and flux tower (Cox et al., 2023b) and radiation station. Measurements from nearby Atmospheric Surface Flux Stations are used to fill temporal gaps in the Met City data streams. SHEBA is a year-long (October 1997–October 1998) drift experiment in the Beaufort Sea. For this study we use SHEBA composite data observations (Persson, 2012). AO2018 is a summer expedition, drifting with an ice floe across the Nansen Basin (31 July–25 September 2018; Vuöllers et al., 2021). ARTofMELT took place in the Fram Strait (7 May–15 June

2023; Tjernström & Zieger, 2025). N-ICE2015 took place in the first half of 2015 north of Svalbard (80–83°N; Cohen et al., 2017). These campaigns together provide high-quality measurements across different regions, seasons/years and ice conditions. All observations are prepared as hourly averages to match the frequency of reanalysis data (see Text S1 in Supporting Information S1 for further details).

2.2. Reanalysis Data

We utilize the ERA5 reanalysis, which is the latest ECMWF reanalysis data set for global weather and climate (Hersbach et al., 2023). ERA5 combines model output with observational data from across the world into a comprehensive and consistent climatic data set using the weather forecast model IFS. It provides hourly atmospheric variables at $0.25^\circ \times 0.25^\circ$ spatial resolution. In this study, we consider the period 1994–2024 over the Arctic (north of 70°N). We extract 16 atmospheric and surface variables (Table S2 in Supporting Information S1) from ERA5, which are relevant to analyze the Arctic SEB. For surface radiation and turbulent fluxes, we follow the convention of the ECMWF, which is positive downwards.

2.3. Neural Network Training, Evaluation and Prediction

ERA5 reanalysis variables are normalized to the same scale (see Table S2 and Text S2 in Supporting Information S1), ensuring reliable and efficient optimization of the NN. We employ a simple feed-forward NN to predict surface fluxes from 16 ERA5 variables. The network consists of five hidden layers of 256 nodes using rectified linear unit activation functions, followed by a linear output layer (Figure S3 in Supporting Information S1). Each model contains 267,777 trainable parameters. The output layer is designed to predict a single bias-corrected variable, and seven separate models are trained, each dedicated to one target variable (see Table S2 and Texts S2–S3 in Supporting Information S1 for further details).

We assess model robustness using a leave-one-campaign-out cross-validation framework, in which each campaign is withheld in turn and used for evaluation while training on the remaining campaigns (Text S4 and Tables S3–S5 in Supporting Information S1). The results show consistent performance across campaigns, with some variability in the magnitude of improvement depending on the withheld data set. Clear improvements over ERA5 across all cases confirm the model's ability to generalize across different Arctic regimes, seasons, and observational conditions. In addition, we use data from N-ICE2015, which is not used for training and from a different year/location, as an independent evaluation (called “testing” in ML). N-ICE2015 spans winter to summer conditions and therefore provides a comprehensive data set for detailed evaluation of model performance. We produce bias-corrected surface fluxes at the ERA5 grid scale (SEBai) by passing ERA5 variables through the NN from the period 1994–2024 over the Arctic Ocean (north of 70°N). SEBai is stored for subsequent analysis. A visual inspection of the bias-corrected data (Figures S4–S6 in Supporting Information S1) exhibits physically plausible patterns, without any unrealistic gradients introduced by the bias-correction. Although each surface flux is predicted independently, we assess the physical consistency of the combined outputs by reconstructing the total SEB from the six SEBai fluxes. The reconstructed total SEB agrees much better with observations than the total SEB from ERA5 (Figure 1; Figure S8 in Supporting Information S1) and does not exhibit any systematic imbalance.

Model performance is quantified by comparing SEBai with N-ICE2015. To ensure robust evaluation, we exclude sensible heat flux values exceeding $\pm 70 \text{ Wm}^{-2}$ prior to analysis ($\sim 5\%$ of data), as the N-ICE2015 sensible heat flux measurements occasionally contained extreme outliers that are likely measurement artifacts. No outliers had to be removed from the training data set. Improvements are assessed against the raw ERA5 fluxes to demonstrate the added value of the NN correction.

3. Results and Discussion

3.1. Biases in ERA5 Surface Fluxes

As a baseline for evaluating the bias correction scheme, we compare hourly ERA5 2 m temperature and surface turbulent and radiative fluxes with the N-ICE2015 campaign data. ERA5 exhibits substantial RMSE values relative to observations for the sensible heat flux (23.1 Wm^{-2}), latent heat flux (13.8 Wm^{-2}), downward long-wave radiation (26.2 Wm^{-2}), net shortwave radiation (18.0 Wm^{-2}), and 2 m temperature (3.8 K; Table S1 in Supporting Information S1). ERA5 is known to systematically overestimate 2 m temperature during winter

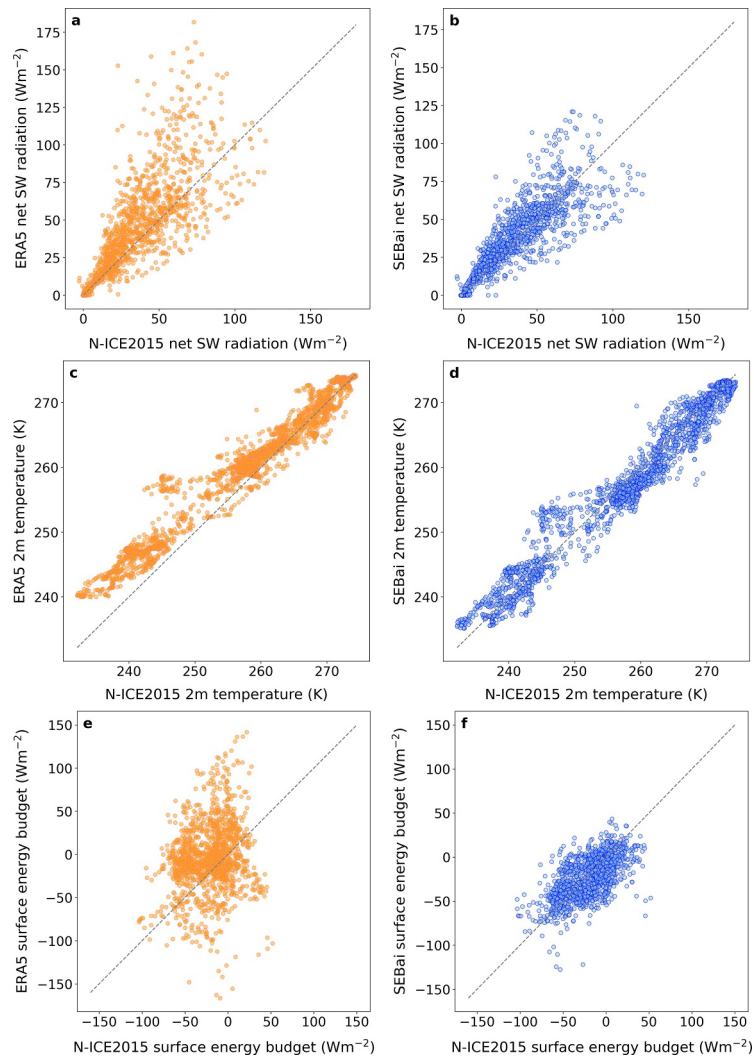


Figure 1. Scatter plots of observed N-ICE2015 hourly surface net shortwave radiation, 2 m temperature and surface energy budget versus ERA5 and SEBai (1:1 reference line).

(Graham et al., 2019; Wang et al., 2019; Yu et al., 2021), which has been attributed to the lack of an insulating snow layer in the model (Batrak & Müller, 2019; Herrmannsdörfer et al., 2023).

We find correlations above 0.8 between ERA5 and observations for 2 m temperature, downwelling and net shortwave radiation and downwelling longwave radiation, variables whose variability is dominated by a strong seasonal cycle (Table S1 in Supporting Information S1). The low correlation coefficients for the remaining variables (net longwave radiation, turbulent heat fluxes and the total SEB) highlight that the reanalysis does not reliably capture observed Arctic boundary-layer processes (Dahlke et al., 2025). The mismatch is particularly striking for the total SEB, defined as the sum of net shortwave and longwave radiation and turbulent heat fluxes. The correlation coefficient of total SEB with observations is 0.18 and the RMSE is 46.4 Wm^{-2} (Table S1 in Supporting Information S1), that is, almost twice the standard deviation of the hourly observed budget itself (25.9 Wm^{-2} , with a mean of -21.2 Wm^{-2}).

3.2. Performance of Machine Learning Bias Correction

The N-ICE2015 campaign is used as an independent data set to assess how our bias correction (SEBai) generalizes outside the training data set.

SEBai is substantially closer to N-ICE2015 observations than ERA5 (Figure 1 and Figure S7 in Supporting Information S1). Hourly RMSE values are reduced by ~40% for net shortwave radiation, ~34% for 2 m temperature, ~32% for sensible heat flux and ~16% for downwelling longwave radiation (Table S1 in Supporting Information S1). We obtain even larger error reductions for daily mean values of net shortwave radiation (~52%), 2 m temperature (~38%), downwelling longwave radiation (~19%) and sensible heat flux (~42%). These results confirm that the bias correction effectively addresses both turbulent and radiative flux errors in the reanalysis.

The wintertime warm bias of ERA5 compared to observations is effectively eliminated in SEBai (~1.3 K; Figure 1c–1d and Figure S8a in Supporting Information S1), which demonstrates that the NN has learned to correct this important bias in the data set. Prior studies have used a linear correction of daily/monthly mean ERA5 temperatures or used satellite observations to partly correct the warm bias in clear-sky situations (Tian et al., 2024; Zampieri et al., 2023). Our bias-correction method works on hourly data under all-sky conditions and makes use of the relationship between the bias in one variable and the state of the atmosphere and boundary layer.

SEBai further produces an improved estimate of the Arctic SEB. For net shortwave radiation, ERA5 captures the observed variability reasonably well (correlation coefficient ≈ 0.87), but demonstrates biases at higher fluxes. SEBai closely reproduces the observed spread with reduced peak values (Figures 1a and 1b), suggesting an improved representation of the surface albedo relative to ERA5. Biases in shortwave radiation and albedo are known deficiencies in ERA5 and other reanalysis data sets, often associated with errors in cloud representation and surface properties (Di Biagio et al., 2021; Graham et al., 2019). For validation, we only include times when ERA5 sea-ice concentration at the nearest grid point to the N-ICE2015 station is more than 80%. At lower concentrations, the measurements on the ice floe may not be representative of the ERA5 grid-box averaged fluxes.

For the total SEB, ERA5 overestimates the frequency of occurrence of both extreme positive and negative values, and hardly shows a notable correlation with observations (correlation coefficient ≈ 0.18 ; Table S1 in Supporting Information S1). This suggests that ERA5 fails to capture the variability of surface energy exchanges (Herrmannsdörfer et al., 2023). In contrast, SEBai captures the variability and magnitude of the observed fluxes with reduced spread (Figure 1 and Figure S8b in Supporting Information S1), although it also produces a few extreme negative values below -100 Wm^{-2} not found in observations. These events have a negligible influence on the climatological mean (-1.67 Wm^{-2} including them vs. -1.66 Wm^{-2} excluding them). The hourly total SEB shows a ~55% reduction in RMSE against N-ICE2015, and the correlation coefficient increases to ~0.64 (Figure 1; Table S1 in Supporting Information S1). For daily values, the error is reduced by ~65% (Figure S9 in Supporting Information S1). Our bias correction thus provides an Arctic-wide data set of the surface energy fluxes that generally captures the observed hourly variability, which is not the case for raw ERA5 data. Since our model was never trained on the total SEB, its good performance for this integrated variable further increases our confidence in the results for individual fluxes.

3.3. Distribution of Net Longwave Radiation

Observational data sets including MOSAiC, SHEBA and N-ICE2015 exhibit a bimodal distribution of net longwave radiation in winter (Graham et al., 2017, 2019; Herrmannsdörfer et al., 2023; Shupe et al., 2026; Figure 2). One mode is near -45 Wm^{-2} corresponding to strong surface cooling under radiatively clear conditions, and another near -5 Wm^{-2} associated with cloudy conditions. The ERA5 distribution does not show the bimodal structure (Bertossa et al., 2025; Dahlke et al., 2025), but a broader spread with a single peak around -20 Wm^{-2} . SEBai reproduces the observed bimodality with peaks near -5 Wm^{-2} , and -45 Wm^{-2} (Figure 2) and thus captures the physically important cloudy and clear states of the Arctic winter boundary layer.

3.4. Seasonal Cycle and Climatology of Surface Fluxes and 2 m Temperature

We investigate the climatology of the Arctic 2 m temperature and surface fluxes over Arctic ice-covered regions (north of 70°N , sea-ice concentration $>80\%$) for the years 1994–2024 using SEBai, and its differences from the ERA5 climatology. Differences may arise from biases in the reanalysis as well as portions of open ocean included in an ERA5 grid cell, where the SEBai value will only be representative of the sea-ice covered portion of the grid cell. In partially ice-covered cells, SEBai represents conditions over sea-ice, whereas ERA5 fluxes reflect grid-cell averages. We therefore focus our evaluation on the ice-covered Arctic Ocean and do not recommend using our bias correction over the marginal ice zone or coastal regions where uncorrected ERA5 fluxes remain the best estimate.

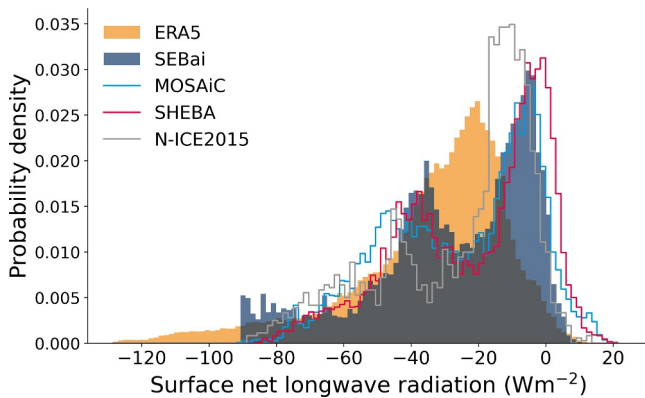


Figure 2. Probability density functions of hourly net longwave radiation during winter (December–February) from observations (solid lines), ERA5 (shaded orange), and SEBai (shaded blue) across the Arctic ($\geq 70^\circ\text{N}$; sea-ice concentration $>80\%$).

Our Arctic-wide bias-corrected estimates show that both wintertime surface cooling and summertime surface heating are dominated by radiative fluxes (Figure 3). In winter (January), the absence of solar radiation leaves the surface dominated by longwave cooling, with downwelling longwave radiation (164 Wm^{-2}) smaller than the upwelling radiation (195 Wm^{-2}). Small positive, that is, downward sensible heat fluxes (5 Wm^{-2}) partly offset this deficit. The resulting net surface cooling corresponds to 22 cm of thermodynamic sea-ice growth. In summer (July), net shortwave radiation dominates the energy balance, leading to net surface warming and an energy gain that corresponds to 49 cm of sea-ice melt.

All data sets qualitatively reproduce the expected seasonal cycles in 2 m temperature, turbulent and radiative fluxes with peaks in summer and minima in winter, but systematic quantitative differences emerge between the ERA5 reanalysis, SEBai, and observations (Figures 4a–4d). MOSAiC and SHEBA observations are included for reference, but are strongly affected by the latitude and summertime cloud cover, and therefore are not necessarily representative of the Arctic Ocean climatology.

Both ERA5 and SEBai capture the pronounced seasonal cycle of downwelling shortwave radiation (Figure 4a), with maxima in June and no shortwave radiation in polar night. SEBai closely follows ERA5 from April–June, but shows an increase of radiation in summer, exceeding 12 Wm^{-2} in July. This suggests a systematic underestimation in ERA5 at a time that is crucial for ice melt. Note that the RMSE of downwelling shortwave radiation is only slightly improved in SEBai (Table S1 in Supporting Information S1), so the true value may well be between the two estimates.

For net shortwave radiation, both ERA5 and SEBai reproduce the expected seasonal cycle, with a peak in June–July (Figure 4b). SEBai absorbs nearly 15 Wm^{-2} less solar energy at the surface in June–July compared to ERA5 due to a higher albedo. Evaluation against N-ICE2015 demonstrates substantial improvement in reproducing net shortwave radiation (Table S1 in Supporting Information S1), indicating that our bias correction provides a more realistic representation of the absorbed shortwave radiation over Arctic sea-ice.

ERA5 produces a wintertime net longwave radiation of around -40 Wm^{-2} (Figure 4d), suggesting an overestimation of surface cooling relative to SEBai and observations of $\sim 10 \text{ Wm}^{-2}$. We attribute this bias to the near-

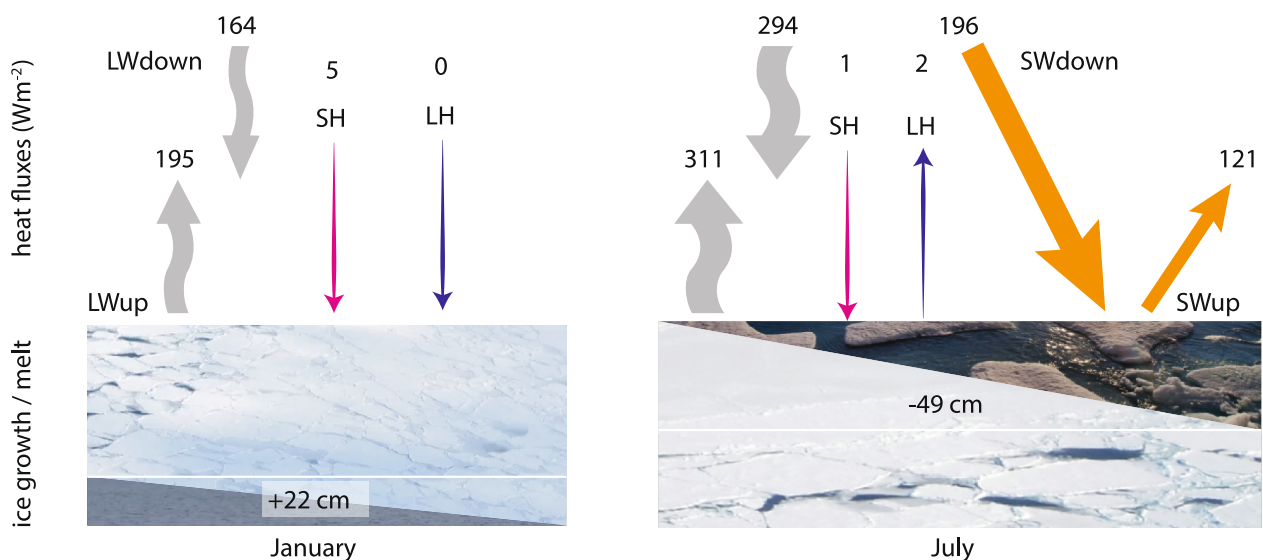


Figure 3. Monthly mean surface energy budget components over Arctic sea-ice ($\geq 70^\circ\text{N}$; sea-ice concentration $>80\%$) in January and July, including longwave (LWup, LWdown), shortwave (SWup, SWdown), sensible (SH) and latent heat (LH) fluxes. Ice-thickness change reflects conversion of the net surface energy budget to ice growth or melt.

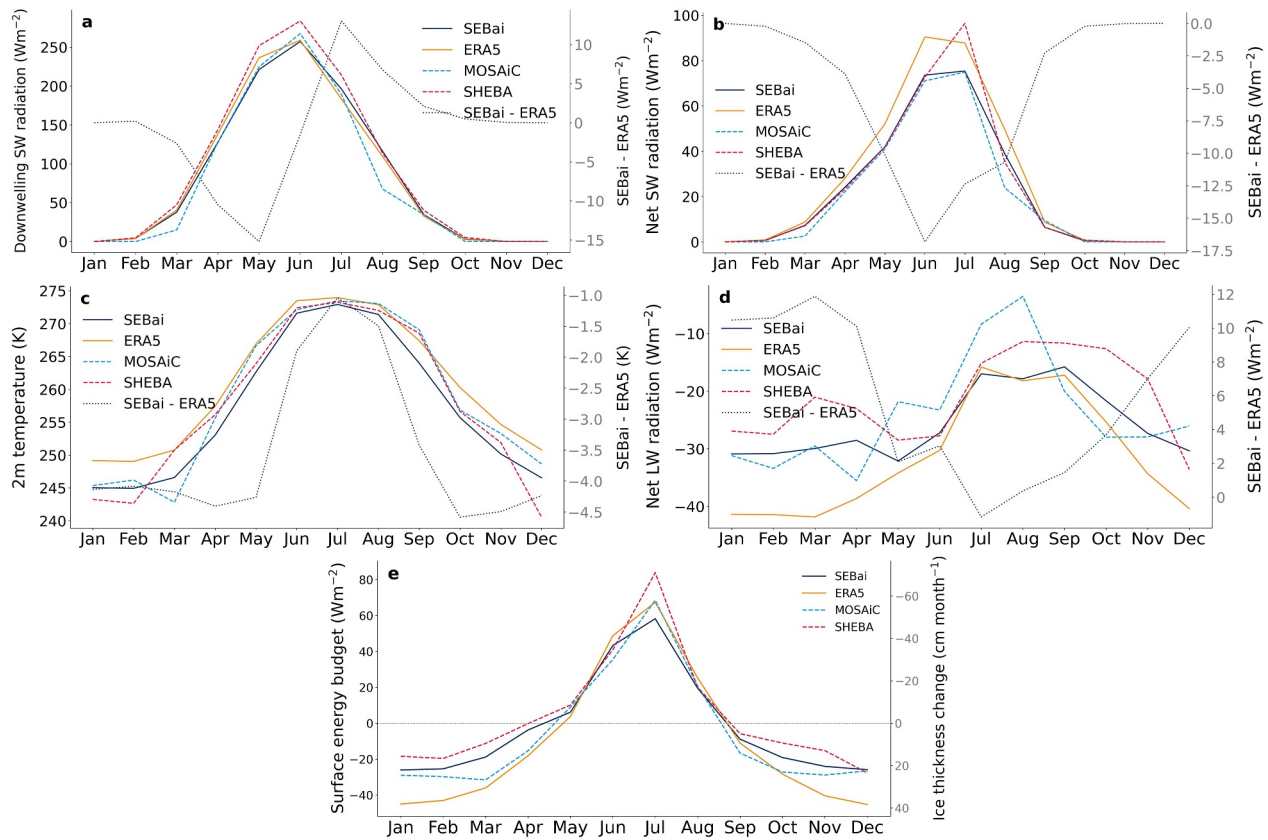


Figure 4. Climatological monthly means of (a) downwelling shortwave, (b) net shortwave radiation, (c) 2 m temperature, (d) net longwave radiation, and (e) surface energy budget and corresponding thermodynamic sea-ice thickness change averaged over Arctic ice-covered regions ($\geq 70^{\circ}N$; sea-ice concentration $>80\%$). Observations (dashed) are compared with SEBai and ERA5 (solid). Panels (a–d) right axis show SEBai–ERA5 differences (dotted). In (e), the left axis shows surface energy budget (positive means energy gain) and the right axis represents ice-thickness change ($cm\ month^{-1}$; positive indicates ice growth).

surface warm bias (lack of snow cover) and the lack of the radiatively opaque or cloudy state in the reanalysis (Di Biagio et al., 2021; Herrmannsdörfer et al., 2023). Both issues are resolved in SEBai, resulting in a more realistic representation of wintertime surface radiative cooling.

The ERA5 warm bias in wintertime 2 m temperatures over Arctic sea-ice peaks at ~ 4 K between November and March (Figure 4c). SEBai substantially reduces this bias and aligns more closely with observations from MOSAiC and SHEBA. During the summer melt season, both ERA5 and SEBai are in better agreement with observations. ERA5 shows a summertime warm bias of ~ 1.5 K that is eliminated in SEBai. Our findings are consistent with wintertime warm biases found in reanalyses over the Arctic and the Weddell Sea pack ice (Herrmannsdörfer et al., 2023; King et al., 2022).

In the total SEB, ERA5 displays a surface energy loss down to $\sim -45 Wm^{-2}$ during winter (November–March). SEBai suggests about half as much cooling, which is in better agreement with observations during MOSAiC and SHEBA (Figure 4e). SEBai suggests weaker net surface heating than ERA5 in summer (June–August). Differences between ERA5 and SEBai are small during the spring and fall transition seasons, which may be due to compensating summer and winter biases. Previous findings confirm that ERA5 and other reanalyses tend to overestimate the amplitude of the seasonal energy cycle and misrepresent the balance between turbulent and radiative fluxes (Graham et al., 2019; Mayer et al., 2019).

Differences between ERA5 and SEBai are largely insensitive to the chosen sea-ice concentration threshold (Figure S10 in Supporting Information S1), especially in winter, which suggests that the correction reflects an improved representation of fluxes over sea-ice rather than open-ocean influences. Our bias-corrected SEB suggests a weaker amplitude of the seasonal cycle than given by ERA5, with weaker wintertime cooling and weaker summertime heating of the ice surface.

3.5. Implications for Sea-Ice Thickness Change

To illustrate the effect of SEB differences on sea-ice, we translate the surface fluxes to thermodynamic changes in sea-ice thickness (Figure 4e). For this conversion, we assume an ice density of 917 kg m^{-3} and a latent heat of fusion of $3.34 \times 10^5 \text{ J kg}^{-1}$. While thermodynamic forcing dominates in observations (SHEBA and MOSAiC), sea-ice thickness is also influenced by dynamical processes such as ice redistribution and ridging. Therefore, we do not expect our estimates to exactly match observed thickness changes.

During winter (October–March), ERA5 suggests Arctic-averaged sea-ice growth rates peaking at $\sim 40 \text{ cm month}^{-1}$ while SEBai produces maximum growth rates just above 20 cm month^{-1} , which aligns more closely with those derived from SHEBA and MOSAiC SEB observations (Raphael et al., 2024; Shupe et al., 2026). The SMOS–CryoSat satellite observations from 2012 to 2024 (European Space Agency, 2023) support these smaller winter sea-ice thickness growth estimates. Satellite estimates and SEBai both suggest sea-ice thickness increases of 80–120 cm for the period October–March (Figure S11 in Supporting Information S1). In contrast, ERA5 consistently implies larger winter sea-ice growth, with thickness changes ranging between ~ 150 and 200 cm . These ERA5 values represent diagnostic thermodynamic estimates based on SEB, not prognostic ice-thickness evolution, since ERA5 does not include fully coupled sea-ice thermodynamics. Both SEBai and ERA5 imply reduced thermodynamic ice growth during spring transition (April–May; Figure 4e). In summer (June–August), ERA5 implies a total melt of around 120 cm , with a maximum melt rate in July of around $-57 \text{ cm month}^{-1}$. SHEBA observations record a similar total summer melt ($\sim 123 \text{ cm}$; Perovich et al., 2003) but stronger July minima ($\sim -71 \text{ cm month}^{-1}$). In contrast, SEBai implies weaker melt ($\sim 102 \text{ cm}$). The sensitivity to the chosen sea-ice concentration threshold (80%, 90%, 95%; Figure S11 in Supporting Information S1) is small, confirming the robustness of these patterns.

The seasonal cycle of the total SEB and sea-ice thickness has been shown to be overestimated in reanalyses, including ERA5 (Mayer et al., 2019). SEBai aligns more closely with observations and produces a more realistic seasonal cycle of thermodynamic ice thickness change consistent with satellite-observed ice thickness changes. Our bias-correction thus provides the basis for a more realistic representation of sea-ice in ice-ocean or coupled reanalyses.

4. Conclusions and Outlook

Leveraging observations through ML provides a powerful means to reduce the systematic biases in ERA5 reanalysis data over Arctic sea-ice. By training a simple NN on variables from ERA5 and major field campaigns, we produce a bias-corrected data set (SEBai) that reveals 50% weaker wintertime surface cooling and weaker summertime surface heating than suggested by ERA5, and eliminates the ERA5 near-surface warm bias of about 4 K in winter and 1.5 K in summer. We expect that the approach can easily be extended to other data-sparse regions, including the Antarctic continent and sea-ice.

Compared to ERA5, we achieve reductions in RMSE against observations by 16%–40% for hourly values of individual fluxes and $\sim 55\%$ for the total SEB. SEBai produces a more realistic climatological seasonal cycle of the total SEB and thermodynamic ice thickness change. Our bias-corrected data reproduce the observed bimodal distribution of net longwave radiation in winter and thus capture the physically important cloudy and clear states of the Arctic boundary layer. The bias correction effectively addresses well-documented deficiencies in ERA5, particularly the representation of albedo, lack of the radiatively opaque or cloudy state and lack of snow cover (Di Biagio et al., 2021; Graham et al., 2019).

The success of the NN in predicting observed fluxes outside of the training data set shows that the surface fluxes over Arctic sea-ice are largely determined by the large-scale state of the atmosphere captured in ERA5. Better parametrizations of the underlying processes than those implemented in the IFS, the model underlying ERA5, are therefore possible.

SEBai allows us to revise climatological estimates of Arctic surface fluxes. Compared to ERA5, we find a damped seasonal cycle driving weaker thermodynamic sea-ice growth in winter and less melt in summer. Together, these changes suggest that the thermodynamic component of Arctic sea-ice evolution is more sensitive to climate change than implied by ERA5.

We expect our bias-corrected data to serve as a new baseline for evaluating climate models, climatological and individual case studies and as forcing for stand-alone sea-ice-ocean models.

Conflict of Interest

The authors declare no conflicts of interest relevant to this study.

Availability Statement

ERA5 reanalysis data are available from the Copernicus Climate Change Service Climate Data Store (Hersbach et al., 2023). The trained neural-network model weights and the curated training data set used to train the model are archived on Zenodo (Hossain et al., 2025). In situ meteorological and surface-flux measurements from the MOSAiC expedition are accessible through the Arctic Data Center (Cox et al., 2023b, 2023c, 2023d, 2023e). SHEBA composite observational data are available via the Arctic Data Center (Persson, 2016). N-ICE2015 surface broadband radiation, atmospheric turbulent fluxes, and surface meteorology data sets are provided by the Norwegian Polar Institute (Hudson et al., 2015, 2016; Walden et al., 2016). Data from the Arctic Ocean 2018 expedition can be obtained from the Bolin Centre Database (Leck et al., 2026), and ARTofMELT data are available through the Bolin Centre Database (Guy et al., 2024a, 2024b). Satellite-derived SMOS–CryoSat Level-4 sea-ice thickness products are available from the European Space Agency (European Space Agency, 2023). The scripts and source data used to produce the figures and tables in this study are archived on Zenodo (Hossain et al., 2025).

References

- Andrews, T., Forster, P. M., & Gregory, J. M. (2009). A surface energy perspective on climate change. *Journal of Climate*, 22(10), 2557–2570. <https://doi.org/10.1175/2008JCLI2759.1>
- Batrak, Y., & Müller, M. (2019). On the warm bias in atmospheric reanalyses induced by the missing snow over Arctic sea-ice. *Nature Communications*, 10(1), 4170. <https://doi.org/10.1038/s41467-019-11975-3>
- Bertossa, C., L'Ecuyer, T., Henderson, D., & McIlhenny, E. (2025). Under-representation of ubiquitous opaque and transmissive arctic atmospheric states in modern reanalyses. *Journal of Climate*, 38(17), 4369–4392. <https://doi.org/10.1175/JCLI-D-24-0490.1>
- Clark, S. K., Brenowitz, N. D., Henn, B., Kwa, A., McGibbon, J., Perkins, W. A., et al. (2022). Correcting a 200 km resolution climate model in multiple climates by machine learning from 25 km resolution simulations. *Journal of Advances in Modeling Earth Systems*, 14(9), e2022MS003219. <https://doi.org/10.1029/2022ms003219>
- Cohen, L., Hudson, S. R., Walden, V. P., Graham, R. M., & Granskog, M. A. (2017). Meteorological conditions in a thinner Arctic sea ice regime from winter to summer during the Norwegian Young Sea ice expedition (N-ICE2015). *Journal of Geophysical Research: Atmospheres*, 122(14), 7235–7259. <https://doi.org/10.1002/2016JD026034>
- Cox, C., Gallagher, M., Shupe, M., Persson, O., Blomquist, B., Grachev, A., et al. (2023b). Met city meteorological and surface flux measurements (level 3 Final), multidisciplinary drifting observatory for the study of arctic climate (MOSAiC), central Arctic, October 2019–September 2020. *Arctic Data Center*. [Dataset]. <https://doi.org/10.18739/A2PV6B83F>
- Cox, C., Gallagher, M., Shupe, M., Persson, O., Blomquist, B., Grachev, A., et al. (2023c). Atmospheric surface flux station #30 measurements (level 3 final), multidisciplinary drifting observatory for the study of arctic climate (MOSAiC), central arctic, October 2019–September 2020. *Arctic Data Center*. [Dataset]. <https://doi.org/10.18739/A2FF3M18K>
- Cox, C., Gallagher, M., Shupe, M., Persson, O., Blomquist, B., Grachev, A., et al. (2023d). Atmospheric surface flux station #40 measurements (level 3 final), multidisciplinary drifting observatory for the study of arctic climate (MOSAiC), central arctic, October 2019–September 2020. *Arctic Data Center*. [Dataset]. <https://doi.org/10.18739/A25X25F0P>
- Cox, C., Gallagher, M., Shupe, M., Persson, O., Blomquist, B., Grachev, A., et al. (2023e). Atmospheric surface flux station #50 measurements (level 3 final), multidisciplinary drifting observatory for the study of arctic climate (MOSAiC), central arctic, October 2019–September 2020. *Arctic Data Center*. [Dataset]. <https://doi.org/10.18739/A2XD0R00S>
- Dahlke, S., Rinke, A., Shupe, M. D., & Cox, C. J. (2025). The two arctic wintertime boundary layer States: Disentangling the role of cloud and wind regimes in reanalysis and observations during MOSAiC. *Atmospheric Science Letters*, 26(4), e1298. <https://doi.org/10.1002/asl.1298>
- Di Biagio, C., Pelon, J., Blanchard, Y., Loyer, L., Hudson, S. R., Walden, V. P., et al. (2021). Toward a better surface radiation budget analysis over sea ice in the high Arctic Ocean: A comparative study between satellite, reanalysis, and local-scale observations. *Journal of Geophysical Research: Atmospheres*, 126(4), e2020JD032555. <https://doi.org/10.1029/2020jd032555>
- European Space Agency. (2023). SMOS–CryoSat Level-4 Sea Ice thickness, version 206. [Dataset]. <https://doi.org/10.57780/sm1-4f787c3>
- Graham, R. M., Cohen, L., Ritzhaupt, N., Segger, B., Graversen, R. G., Rinke, A., et al. (2019). Evaluation of six atmospheric reanalyses over Arctic sea ice from winter to early summer. *Journal of Climate*, 32(14), 4121–4143. <https://doi.org/10.1175/jcli-d-18-0643.1>
- Graham, R. M., Rinke, A., Cohen, L., Hudson, S. R., Walden, V. P., Granskog, M. A., et al. (2017). A comparison of the two Arctic atmospheric winter states observed during N-ICE2015 and SHEBA. *Journal of Geophysical Research: Atmospheres*, 122(11), 5716–5737. <https://doi.org/10.1002/2016JD025475>
- Granskog, M. A., Fer, I., Rinke, A., & Steen, H. (2018). Atmosphere-ice-ocean-ecosystem processes in a thinner arctic sea ice regime: The Norwegian young sea ICE (N-ICE2015) expedition. *Journal of Geophysical Research: Oceans*, 123(3), 1586–1594. <https://doi.org/10.1002/2017jc013328>
- Guy, H., Brooks, I., Murto, S., Karalis, M., & Tjernström, M. (2024a). Ice station surface meteorology and radiation data from expedition ARTofMELT, Arctic Ocean, 2023, dataset version 1. *Bolin Centre Database*. [Dataset] <https://doi.org/10.17043/oden-artofmelt-2023-surface-meteorology-ice-station-1>

Acknowledgments

We thank all scientists, logistics personnel and crew involved in the MOSAiC, SHEBA, N-ICE2015, AO2018 and ARTofMELT expeditions. We acknowledge the open data policy of the MOSAiC, SHEBA, N-ICE, AO2018 and ARTofMELT projects. We are grateful to ECMWF for making available the ERA5 product. This research was supported by the Alfred Wegener Institute (AWI) through the DataHub Information Infrastructure program and by the European Union (ERC A3M-transform, Grant agreement no. 101076205). This work was also supported by Helmholtz Association's Initiative and Networking Fund through Helmholtz AI (Grant ZT-I-PF-5-01). Computational resources were provided by the Deutsches Klimarechenzentrum (DKRZ) under project ID AIM, as granted by its Scientific Steering Committee (WLA). In situ data used in this article were produced as part of the international MOSAiC expedition with tag MOSAiC20192020 and Project_ID: AWI_PS122_00. Some radiation data were collected by the Atmospheric Radiation Measurement User Facility, a DOE Office of Science user facility operated by the Biological and Environmental Research program. The field expeditions were supported by the NOAA Global Ocean Monitoring and Observing Program (FundRef 10.13039/100018302), NOAA Physical Science Laboratory (NA22OAR4320151), the National Science Foundation (OPP-1724551), Department of Energy Atmospheric System Research Program (DE-SC0021341), the Swedish Polar Research Secretariat, the Knut and Alice Wallenberg Foundation (contract: 2016.0024), and the Swedish Research Council's National Research Infrastructure (contract: 2021-00153), UK Natural Environment Research Council (NE/R009686/1 and NE/X000087/1), the Atmospheric Measurements and Observations Facility (AMOF) of the UK National Centre for Atmospheric Science (NCAS), the NERC project (Grant number: NE/X000087/1), the Centre of Ice, Climate and Ecosystems (ICE) at the Norwegian Polar Institute (N-ICE project) and the Ministry of Climate and Environment and the Ministry of Foreign Affairs of Norway. We thank Lars Kaleschke (AWI) for providing the SMOS–CryoSat sea-ice thickness data, and Lana Cohen for her contributions to the atmospheric measurements during N-ICE2015. Pictures by Fabian Reiser, Jan-Marcus Nasse, and Michael Tjernström, distributed via imageo.edu.eu, were used to produce Figure 3. Open Access funding enabled and organized by Projekt DEAL.

- Guy, H., Brooks, I., Murto, S., Karalis, M., & Tjernström, M. (2024b). Ice station micrometeorological data from expedition ARTofMELT, Arctic Ocean, 2023, dataset version 1. *Bolin Centre Database*. [Dataset] <https://doi.org/10.17043/oden-artofmelt-2023-micrometeorology-ice-station-1>
- Herrmannsdörfer, L., Müller, M., Shupe, M. D., & Rostosky, P. (2023). Surface temperature comparison of the arctic winter MOSAiC observations, ERA5 reanalysis, and MODIS satellite retrieval. *Elementa: Science of the Anthropocene*, 11(1), 00085. <https://doi.org/10.1525/elementa.2022.00085>
- Hersbach, H., Bell, B., Berrisford, P., Biavati, G., Horányi, A., Muñoz Sabater, J., et al. (2023). ERA5 hourly data on single levels from 1940 to present. *Copernicus Climate Change Service (C3S) Climate Data Store (CDS)*. [Dataset]. <https://doi.org/10.24381/cds.adbb2d47>
- Hersbach, H., Bell, B., Berrisford, P., Hirahara, S., Horányi, A., Muñoz-Sabater, J., et al. (2020). The ERA5 global reanalysis. *Quarterly Journal of the Royal Meteorological Society*, 146(730), 1999–2049. <https://doi.org/10.1002/qj.3803>
- Hossain, A., Keil, P., Grover, H., Brooks, I. M., Cox, C. J., Gallagher, M. R., et al. (2025). Bias-correcting the reanalysis arctic surface energy budget and near-surface temperature with machine learning. In *Geophysical research letters*. Zenodo. [Collection]. <https://doi.org/10.5281/zenodo.17964954>
- Hudson, S. R., Cohen, L., & Walden, V. (2015). N-ICE2015 surface meteorology. *Norwegian Polar Institute*. [Dataset]. <https://doi.org/10.21334/NPOLAR.2015.056A61D1>
- Hudson, S. R., Cohen, L., & Walden, V. P. (2016). N-ICE2015 surface broadband radiation data. *Norwegian Polar Institute*. [Dataset]. <https://doi.org/10.21334/NPOLAR.2016.A89CB766>
- Istomina, L., Marks, H., Huntemann, M., Heygster, G., & Spreen, G. (2020). Improved cloud detection over sea ice and snow during arctic summer using MERIS data. *Atmospheric Measurement Techniques Discussions*, 2020(12), 1–22. <https://doi.org/10.5194/amt-13-6459-2020>
- Jakobson, E., Vihma, T., Palo, T., Jakobson, L., Keernik, H., & Jaagus, J. (2012). Validation of atmospheric reanalyses over the central Arctic Ocean. *Geophysical Research Letters*, 39(10). <https://doi.org/10.1029/2012gl015191>
- Jung, T., Gordon, N. D., Bauer, P., Bromwich, D. H., Chevallier, M., Day, J. J., et al. (2016). Advancing polar prediction capabilities on daily to seasonal time scales. *Bulletin of the American Meteorological Society*, 97(9), 1631–1647. <https://doi.org/10.1175/BAMS-D-14-00246.1>
- King, J. C., Marshall, G. J., Colwell, S., Arndt, S., Allen-Sader, C., & Phillips, T. (2022). The performance of the ERA-interim and ERA5 atmospheric reanalyses over Weddell Sea pack ice. *Journal of Geophysical Research: Oceans*, 127(9), e2022JC018805. <https://doi.org/10.1029/2022JC018805>
- Lawrence, H., Bormann, N., Sandu, I., Day, J., Farman, J., & Bauer, P. (2019). Use and impact of arctic observations in the ECMWF numerical weather prediction system. *Quarterly Journal of the Royal Meteorological Society*, 145(725), 3432–3454. <https://doi.org/10.1002/qj.3628>
- Leck, C., Matrai, P., Achtert, P., Adams, M., Baccarini, A., Brooks, B., et al. (2026). Data from expedition Arctic Ocean 2018 (Version 5) [Dataset]. *Bolin Centre Database*. <https://doi.org/10.17043/oden-ao-2018-expedition-5>
- Li, H., Zhang, Y., Lei, H., & Hao, X. (2023). Machine learning-based bias correction of precipitation measurements at high altitude. *Remote Sensing*, 15(8), 2180. <https://doi.org/10.3390/rs15082180>
- Li, Z., Shen, H., Weng, Q., Zhang, Y., Dou, P., & Zhang, L. (2022). Cloud and cloud shadow detection for optical satellite imagery: Features, algorithms, validation, and prospects. *ISPRS Journal of Photogrammetry and Remote Sensing*, 188, 89–108. <https://doi.org/10.1016/j.isprsjprs.2022.03.020>
- Mallet, M. D., Alexander, S. P., Protat, A., & Fiddes, S. L. (2023). Reducing Southern Ocean shortwave radiation errors in the ERA5 reanalysis with machine learning and 25 years of surface observations. *Artificial Intelligence for the Earth Systems*, 2(2), e220044. <https://doi.org/10.1117/5/aies-d-22-0044.1>
- Mayer, M., Tietsche, S., Haimberger, L., Tsubouchi, T., Mayer, J., & Zuo, H. (2019). An improved estimate of the coupled arctic energy budget. *Journal of Climate*, 32(22), 7915–7934. <https://doi.org/10.1175/JCLI-D-19-0233.1>
- Moghim, S., & Bras, R. L. (2017). Bias correction of climate modeled temperature and precipitation using artificial neural networks. *Journal of Hydrometeorology*, 18(7), 1867–1884. <https://doi.org/10.1175/jhm-d-16-0247.1>
- Müller, R., & Pfeifroth, U. (2022). Remote sensing of solar surface Radiation—A reflection of concepts, applications and input data based on experience with the effective cloud albedo. *Atmospheric Measurement Techniques*, 15(5), 1537–1561. <https://doi.org/10.5194/amt-15-1537-2022>
- Niazkar, M., Piraei, R., Menapace, A., Dhawan, P., Torre, D. D., Larcher, M., & Righetti, M. (2024). Bias correction of ERA5-Land temperature data using standalone and ensemble machine learning models: A case of northern Italy. *Journal of Water and Climate Change*, 15(1), 271–283. <https://doi.org/10.2166/wcc.2023.669>
- Perovich, D. K., Grenfell, T. C., Richter-Menge, J. A., Light, B., Tucker, W. B., III., & Eicken, H. (2003). Thin and thinner: Sea ice mass balance measurements during SHEBA. *Journal of Geophysical Research*, 108(C3). <https://doi.org/10.1029/2001jc001079>
- Persson, P. O. G. (2012). Onset and end of the summer melt season over sea ice: Thermal structure and surface energy perspective from SHEBA. *Climate Dynamics*, 39(6), 1349–1371. <https://doi.org/10.1007/s00382-011-1196-9>
- Persson, P. O. G. (2016). SHEBA composite data observations. *Arctic Data Center*. [Dataset]. <https://doi.org/10.5065/D6PN93R6>
- Persson, P. O. G., Fairall, C. W., Andreas, E. L., Guest, P. S., & Perovich, D. K. (2002). Measurements near the atmospheric surface flux group tower at SHEBA: Near-surface conditions and surface energy budget. *Journal of Geophysical Research*, 107(C10), SHE-21. <https://doi.org/10.1029/2000JC000705>
- Pithan, F., Ackerman, A., Angevine, W. M., Hartung, K., Ickes, L., Kelley, M., et al. (2016). Select strengths and biases of models in representing the arctic winter boundary layer over sea ice: The larform 1 single column model intercomparison. *Journal of Advances in Modeling Earth Systems*, 8(3), 1345–1357. <https://doi.org/10.1002/2016MS000630>
- Rantanen, M., Karpechko, A. Y., Lipponen, A., Nordling, K., Hyvärinen, O., Ruosteenoja, K., et al. (2022). The arctic has warmed nearly four times faster than the globe since 1979. *Communications Earth & Environment*, 3(1), 168. <https://doi.org/10.1038/s43247-022-00498-3>
- Raphael, I. A., Perovich, D. K., Polashenski, C. M., Clemens-Sewall, D., Itkin, P., Lei, R., et al. (2024). Sea ice mass balance during the MOSAiC drift experiment: Results from manual ice and snow thickness gauges. *Elementa: Science of the Anthropocene*, 12(1), 00040. <https://doi.org/10.1525/elementa.2023.00040>
- Sandu, I., Beljaars, A., Bechtold, P., Mauritsen, T., & Balsamo, G. (2013). Why is it so difficult to represent stably stratified conditions in numerical weather prediction (NWP) models? *Journal of Advances in Modeling Earth Systems*, 5(2), 117–133. <https://doi.org/10.1002/jame.20013>
- Serreze, M. C., Holland, M. M., & Stroeve, J. (2007). Perspectives on the Arctic's shrinking sea-ice cover. *Science*, 315(5818), 1533–1536. <https://doi.org/10.1126/science.1139426>
- Shupe, M. D., Persson, P. O. G., Cox, C. J., Gallagher, M. R., Solomon, A., Sledd, A., et al. (2026). The two radiative states of the arctic atmosphere and their impacts on the surface energy budget of sea ice. *Elementa: Science of the Anthropocene*, 14(1), 00100. <https://doi.org/10.1525/elementa.2025.00100>

- Shupe, M. D., Rex, M., Blomquist, B., Persson, P. O. G., Schmale, J., Uttal, T., et al. (2022). Overview of the MOSAiC expedition: Atmosphere. *Elementa: Science of the Anthropocene*, 10(1), 00060. <https://doi.org/10.1525/elementa.2021.00060>
- Sun, H., Yao, T., Su, F., He, Z., Tang, G., Li, N., et al. (2022). Corrected ERA5 precipitation by machine learning significantly improved flow simulations for the third pole basins. *Journal of Hydrometeorology*, 23(10), 1663–1679. <https://doi.org/10.1175/jhm-d-22-0015.1>
- Taylor, P. C., Boeke, R. C., Boisvert, L. N., Feldl, N., Henry, M., Huang, Y., et al. (2022). Process drivers, inter-model spread, and the path forward: A review of amplified arctic warming. *Frontiers in Earth Science*, 9, 758361. <https://doi.org/10.3389/feart.2021.758361>
- Tian, T., Yang, S., Høyer, J. L., Nielsen-Englyst, P., & Singha, S. (2024). Cooler arctic surface temperatures simulated by climate models are closer to satellite-based data than the ERA5 reanalysis. *Communications Earth & Environment*, 5(1), 111. <https://doi.org/10.1038/s43247-024-01276-z>
- Tjernström, M., & Zieger, P. (2025). *ARTofMELT 2023: Expedition report*. Swedish Polar Research Secretariat. Retrieved from <https://www.polar.se/en/expeditions/expedition-reports>
- Uttal, T., Curry, J. A., McPhee, M. G., Perovich, D. K., Moritz, R. E., Maslanik, J. A., et al. (2002). Surface heat budget of the Arctic Ocean. *Bulletin of the American Meteorological Society*, 83(2), 255–276. [https://doi.org/10.1175/1520-0477\(2002\)083<0255:shbota>2.3.co;2](https://doi.org/10.1175/1520-0477(2002)083<0255:shbota>2.3.co;2)
- Vüllers, J., Achtert, P., Brooks, I. M., Tjernström, M., Prytherch, J., Burzik, A., & Neely, III, R. (2021). Meteorological and cloud conditions during the Arctic Ocean 2018 expedition. *Atmospheric Chemistry and Physics*, 21(1), 289–314. <https://doi.org/10.5194/acp-21-289-2021>
- Walden, V. P., Murphy, S., Hudson, S. R., & Cohen, L. (2016). N-ICE2015 atmospheric turbulent fluxes. *Norwegian Polar Institute*. [Dataset]. <https://doi.org/10.21334/NPOLAR.2017.298013B7>
- Wang, C., Graham, R. M., Wang, K., Gerland, S., & Granskog, M. A. (2019). Comparison of ERA5 and ERA-interim near-surface air temperature, snowfall and precipitation over arctic sea ice: Effects on sea ice thermodynamics and evolution. *The Cryosphere*, 13(6), 1661–1679. <https://doi.org/10.5194/tc-13-1661-2019>
- Werneck, A., Notz, D., Kern, S., & Lavergne, T. (2024). Estimating the uncertainty of sea-ice area and sea-ice extent from satellite retrievals. *The Cryosphere*, 18(5), 2473–2486. <https://doi.org/10.5194/tc-18-2473-2024>
- Yu, Y., Xiao, W., Zhang, Z., Cheng, X., Hui, F., & Zhao, J. (2021). Evaluation of 2-m air temperature and surface temperature from ERA5 and ERA-I using buoy observations in the arctic during 2010–2020. *Remote Sensing*, 13(14), 2813. <https://doi.org/10.3390/rs13142813>
- Zampieri, L., Arduini, G., Holland, M., Keeley, S. P., Mogensen, K., Shupe, M. D., & Tietsche, S. (2023). A machine learning correction model of the winter clear-sky temperature bias over the arctic sea ice in atmospheric reanalyses. *Monthly Weather Review*, 151(6), 1443–1458. <https://doi.org/10.1175/MWR-D-22-0130.1>

References From the Supporting Information

- Hastie, T., Tibshirani, R., & Friedman, J. (2009). *The elements of statistical learning: Data mining, inference, and prediction*. Springer. 2nd ed. <https://doi.org/10.1007/978-0-387-84858-7>
- Huber, P. J. (1964). Robust estimation of a location parameter. *The Annals of Mathematical Statistics*, 35(1), 73–101. <https://doi.org/10.1214/aom/s/1177703732>
- Ioffe, S., & Szegedy, C. (2015). Batch normalization: Accelerating deep network training by reducing internal covariate shift. In *Proceedings of the 32nd international conference on machine learning (ICML)* (pp. 448–456).
- Kuhn, M., & Silge, J. (2022). *Tidy modeling with R*. Springer. 1st ed. <https://doi.org/10.1007/978-1-4842-7164-6>
- Prytherch, J., Yelland, M. J., Brooks, I. M., Tupman, D. J., Pascal, R. W., Moat, B. I., & Norris, S. J. (2015). Motion-correlated flow distortion and wave-induced biases in air–sea flux measurements from ships. *Atmospheric Chemistry and Physics*, 15(18), 10619–10629. <https://doi.org/10.5194/acp-15-10619-2015>
- Prytherch, J., Brooks, I. M., Crill, P. M., Thornton, B. F., Salisbury, D. J., Tjernström, M., et al. (2017). Direct determination of the air–sea CO₂ gas transfer velocity in arctic sea ice regions. *Geophysical Research Letters*, 44(8), 3770–3778. <https://doi.org/10.1002/2017GL073593>
- Spren, G., Kaleschke, L., & Heygster, G. (2008). Sea ice remote sensing using AMSR-E 89-GHz channels. *Journal of Geophysical Research*, 113(C2). <https://doi.org/10.1029/2005JC003384>
- Srivastava, N., Hinton, G., Krizhevsky, A., Sutskever, I., & Salakhutdinov, R. (2014). Dropout: A simple way to prevent neural networks from overfitting. *Journal of Machine Learning Research*, 15(1), 1929–1958.
- Walden, V. P., Hudson, S. R., Cohen, L., Murphy, S. Y., & Granskog, M. A. (2017). Atmospheric components of the surface energy budget over young sea ice: Results from the N-ICE2015 campaign. *Journal of Geophysical Research: Atmospheres*, 122(16), 8427–8446. <https://doi.org/10.1002/2016JD026091>
- Cox, C. J., Gallagher, M. R., Shupe, M. D., Persson, P. O. G., Solomon, A., Fairall, C. W., et al. (2023a). Continuous observations of the surface energy budget and meteorology over the arctic sea ice during MOSAiC. *Scientific Data*, 10(1), 519. <https://doi.org/10.1038/s41597-023-02415-5>
- Kingma, D. P., & Ba, J. (2015). Adam: A method for stochastic optimization. In *Conference paper at the 3rd international conference for learning representations*. arXiv:1412.6980ss.